

Macromolecules

Volume 31, Number 14

July 14, 1998

© Copyright 1998 by the American Chemical Society

Chirality Induction in Cyclocopolymerization. 9. Characterization of Chirality Induction during the Cyclocopolymerizations of (2*S*,3*S*)-2,3-Butanediyl, (2*S*,4*S*)-2,4-Pentanediyl, and (2*S*,5*S*)-2,5-Hexanediyl Bis(4-vinylbenzoate)s with Styrene

Makoto Obata,[†] Takahiro Uesaka,[†] Kazuaki Yokota,^{*,†} and Toyoji Kakuchi[‡]

Division of Molecular Chemistry, Graduate School of Engineering, Hokkaido University, Sapporo 060, Japan, and Division of Bioscience, Graduate School of Environmental Earth Science, Hokkaido University, Sapporo 060, Japan

Received December 31, 1997; Revised Manuscript Received April 28, 1998

ABSTRACT: Optically active poly(methyl 4-vinylbenzoate-*co*-styrene)s (**3a–c**) were synthesized through the cyclocopolymerizations of (2*S*,3*S*)-2,3-butanediyl, (2*S*,4*S*)-2,4-pentanediyl, and (2*S*,5*S*)-2,5-hexanediyl bis(4-vinylbenzoate)s (**1a**, **1b**, and **1c**, respectively) with styrene. The extent of chirality induction increased in the order of **1a** \cong **1c** < **1b**, and the cyclized units predominately possessed an (*R,R*)-configuration. The MM2 calculation derived the conformer distributions, in which monomers **1a** and **1b** predominately had a counterclockwise gauche form ("g⁻") and a combination of trans form and clockwise gauche form ("tg⁺"), respectively. Monomer **1c** had a wide distribution into "tg⁺g⁺", "g⁺tg⁺", and "ttt" forms because of flexibility. The semiempirical molecular orbital calculations were performed for the model reaction of the radical cyclization. The calculated population difference between (*R,R*)- and (*S,S*)-configurations indicated that the template in **1b** was more effective for the chirality induction than that in **1a**, similar to the experimental results.

Introduction

Various types of optically active polymers have been synthesized, and the polymers having chirality in the main chain are classified into two categories, namely, configurationally and conformationally chiral polymers.¹ Cyclocopolymerization capable of forming the chiral diad affords a useful method for the former polymers.² We have reported the cyclocopolymerization of dimethacrylate^{2d} and bis(4-vinylbenzoate)^{2e–l} having chiral templates with styrene to yield optically active poly-(methyl methacrylate-*co*-styrene) and poly(methyl 4-vinylbenzoate-*co*-styrene). The occurrence of chirality was attributable to the intramolecular cyclization to form an enantiomeric racemo configuration. The template transmitted its chirality to the main chain during the cyclization.

Our continuous interest, therefore, is to clarify the structural characteristics and the efficiency of the template on the chirality induction. Several types of templates, such as carbohydrates and synthetic chiral diols, were used for examining the distance, torsion angle, rotational freedom, steric crowding between two functional groups, and the number of chiral centers in a template. A method estimating the efficiency of the template, however, has yet to be found, and it is desirable to study the quantitative treatment for chirality induction.³

In this paper, the chirality induction in the cyclocopolymerization was examined for the bis(4-vinylbenzoate)s derived from 1,2-, 1,3-, and 1,4-diols, namely, (2*S*,3*S*)-2,3-butanediol, (2*S*,4*S*)-2,4-pentanediol, and (2*S*,5*S*)-2,5-hexanediol, and further confirmed by use of a computational study. To characterize the chirality induction, the heat of formation at the transition state of the radical cyclization, which is a model reaction for cyclocopolymerization, was estimated using a semiempirical molecular orbital calculation. The calculated results elucidated the characteristics of chirality induc-

* To whom correspondence should be addressed. Telephone and fax: international code + 81-11-706-6602. E-mail: yokota@poly.eng.hokudai.ac.jp.

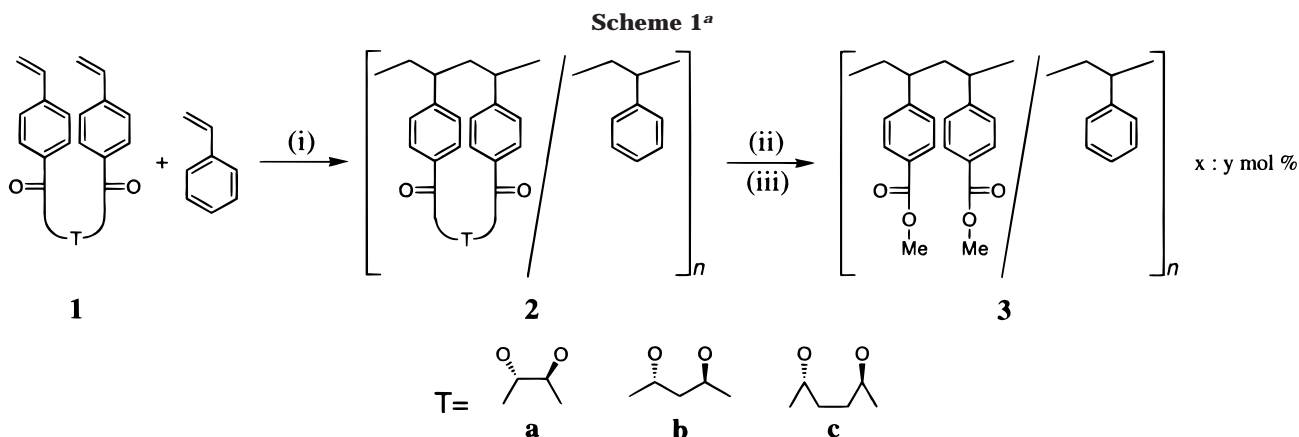
[†] Graduate School of Engineering, Hokkaido University.

[‡] Graduate School of Environmental Earth Science.

Table 1. Copolymerizations of Bis(4-vinylbenzoate)s (**1a–c**) with Styrene to form Poly(methyl 4-vinylbenzoate-*co*-styrene) (**3a–c**)

monomer	polymer 2 ^a							polymer 3 ^b		
	<i>F</i> ₁ ^c	time, h	yield, %	<i>f</i> ₁ ^d	<i>f</i> _c ^e	<i>M</i> _n (<i>M</i> _w / <i>M</i> _n) ^f	[α] ₄₃₅ , ^g deg	yield, %	<i>M</i> _n (<i>M</i> _w / <i>M</i> _n) ^f	[α] ₄₃₅ , ^g deg
1a ^h	0.9	2.5	24	0.99	0.86	22900 (3.41)	+278	27	21400 (1.72)	−1
	0.7	3.5	28	0.79	0.89	18700 (1.76)	+313	46	14400 (1.42)	−2
	0.5	3.0	9	0.66	0.89	10700 (1.78)	+307	73	9200 (1.76)	−3
	0.3	5.5	25	0.51	0.94	7900 (1.62)	+319	56	7200 (1.53)	−5
	0.1	12.5	14	0.30	0.94	3900 (1.67)	+252	61	3800 (1.48)	−8
1b ⁱ	0.9	1.0	22	0.97		37000 (1.73)	+434	32	28800 (1.92)	0
	0.7	1.8	24	0.89		31300 (1.89)	+394	41	21800 (1.98)	−9
	0.5	2.5	22	0.79		20900 (2.25)	+385	72	15700 (2.12)	−20
	0.3	4.0	21	0.61		9000 (2.09)	+354	64	6900 (2.16)	−36
	0.2	5.0	22	0.49		5000 (1.60)	+319	70	5500 (1.47)	−46
1c	0.9	1.5	16	0.95	0.85	19200 (2.28)	+218	58	22800 (2.11)	0
	0.7	1.7	18	0.77	0.90	12500 (2.03)	+268	47	11700 (1.81)	−4
	0.5	2.5	17	0.68	0.88	10000 (1.96)	+275	68	10500 (1.58)	−7
	0.3	3.5	11	0.56	0.90	7300 (1.67)	+263	80	7300 (1.50)	−15
	0.1	8.0	11	0.29	0.95	4100 (1.33)	+218	80	4300 (1.54)	−24

^a Solvent, toluene; [**1** + styrene] = 0.1 mol·L^{−1}; [AIBN] = 6.1 mmol·L^{−1}; temp, 60 °C. ^b Prepared from polymer **2** through hydrolysis using KOH in aqueous MeOH and then treatment with diazomethane. ^c Mole fraction of *M*₁ in the monomer feed. ^d Mole fraction of *M*₁ unit in the polymer; determined by ¹H and quantitative ¹³C NMR spectra. ^e Extent of cyclization determined by quantitative ¹³C NMR spectra. ^f Determined by GPC using a polystyrene standard. ^g Measured in CHCl₃ at 23 °C (*c* = 1.0). ^h Data from ref 2k. ⁱ Data from ref 2g.



^a Conditions: (i) AIBN, toluene, 60 °C; (ii) KOH, MeOH, reflux; (iii) CH₂N₂, Et₂O.

tion, in particular, the determination process of chiral centers during the polymerization.

Experimental Section

Measurements. ¹H and ¹³C NMR spectra were recorded using JEOL JNM-EX270 and JNM-A400II instruments. Quantitative ¹³C NMR spectra were obtained at 30 °C in CDCl₃ (100 mg/mL; delay time 7.0 s; inverse gated decoupling). The molecular weight of the resulting polymers was measured by gel permeation chromatography (GPC) in tetrahydrofuran with a Jasco Intelligent HPLC system (880-PU pump and 830-R1 detector) equipped with three polystyrene columns (Shodex KF-804L). The number-averaged molecular weight (*M*_n) was calculated on the basis of a polystyrene calibration. Optical rotations were measured with a Jasco DIP-140 digital polarimeter. CD spectra were measured at 24 °C in hexafluoro-2-propanol (HFIP) with a 0.5 cm path length using a Jasco J-720 spectropolarimeter.

Materials. Toluene was refluxed over sodium benzo-phenone ketyl and distilled just before use. α,α'-Azobisisobutyronitrile (AIBN) was recrystallized from methanol. HFIP was donated by Central Glass Co. and used without further purification.

(2*S*,3*S*)-2,3-Butanediyl and (2*S*,4*S*)-2,4-Pentanediiyl Bis(4-vinylbenzoate)s (1a** and **1b**).** The procedures are reported in previous papers.^{2k,g}

(2*S*,5*S*)-2,5-Hexanediiyl Bis(4-vinylbenzoate) (1c**).** The procedure is analogous to those reported in previous papers.^{2k,g} To a solution of (2*S*,5*S*)-2,5-hexanediol⁴ (4.3 g, 0.036 mol) in

dry pyridine (200 mL) was gradually added 4-vinylbenzoyl chloride (18.3 g, 0.11 mol) at 5–10 °C, and then the mixture was heated at 80 °C with stirring for 4 h. When the solution was cooled and diluted with water, the resulting mixture was stirred further for 1 h and extracted with dichloromethane. After removal of the solvent under reduced pressure, the residue was purified by squat column chromatography on alumina with hexane/ether (volume ratio 4:1), followed by recrystallization from hexane to give 8.5 g of **1c** (yield 62%) as a white powder. [α]_D²⁴ = +23.6°, [α]₄₃₅²⁴ = +60.2° (*c* 1.0, CHCl₃). ¹H NMR (270 MHz, CDCl₃): δ (ppm) = 7.99 (d, ³*J* = 8.2 Hz, 4H, Ar), 7.45 (d, ³*J* = 8.2 Hz, 4H, Ar), 6.75 (dd, *J*_{trans} = 17.5 Hz, *J*_{cis} = 10.9 Hz, 2H, =CH–), 5.85 (d, *J*_{trans} = 17.5 Hz, 2H, =CH₂), 5.37 (d, *J*_{cis} = 10.9 Hz, 2H, =CH₂), 5.16–5.23 (m, 2H, CH), 1.94–1.66 (m, 4H, CH₂), 1.36 (d, 6.3 Hz, 6H, CH₃). ¹³C NMR (67.8 MHz, CDCl₃): δ (ppm) = 165.9 (C=O), 141.8, 129.8, 126.0 (arom), 136.0 (–CH=), 116.4 (=CH₂), 71.1 (CH), 31.8 (CH₂), 20.0 (CH₃). Anal. Calcd for C₂₄H₂₆O₄ (378.5): C 76.17; H 6.92. Found: C 76.10; H 6.98.

Cyclocopolymerization. The cyclocopolymerization of **1** with styrene was carried out using AIBN in toluene at 60 °C. After an appropriate time, the polymerization mixture was poured into methanol and the precipitate was filtered. The obtained white powder was purified by reprecipitation with chloroform–methanol and dried in vacuo.

Poly(methyl 4-vinylbenzoate-*co*-styrene) (3**).** The removal of the chiral template from **2** was carried out using methanolic KOH. After neutralization with hydrochloric acid, the solution was dialyzed using a cellophane tube and later

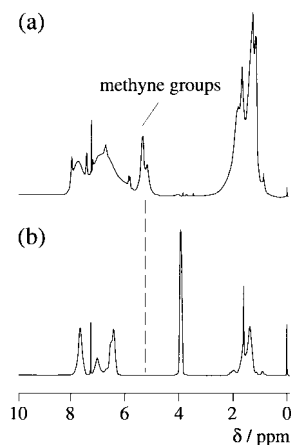


Figure 1. ^1H NMR spectra of (a) **2c** ($f_1 = 0.62$) and (b) **3c** ($f_1 = 0.62$)

concentrated by freeze-drying. The hydrolyzed copolymers were treated with diazomethane in benzene/ether, whereupon copolymers **3** were obtained.^{2d} The procedures of dialysis and freeze-drying lowered the yields of **3** as shown in Table 1.

Computational Procedure. The molecular mechanics and molecular orbital calculations were carried out using MM2⁵ and MOPAC ver 6.01⁶ implemented in the ANCHOR II package. The transition state geometry was optimized using the NLLSQ algorithm. The system was characterized as a transition state by the presence of only one negative force constant in the Hessian matrix of the normal coordinate analysis.

Results and Discussion

Cyclocopolymerization. Radical copolymerizations of (2*S*,3*S*)-2,3-butanediyl, (2*S*,4*S*)-2,4-pentanedyl, and (2*S*,5*S*)-2,5-hexanedyl bis(4-vinylbenzoate)s (**1a**, **1b**, and **1c**, respectively) (M_1) with styrene (M_2) were carried out using AIBN in toluene at 60 °C (Scheme 1 and Table 1). The polymerization systems were homogeneous and the resulting copolymers (**2a**, **2b**, and **2c**) were soluble in chloroform and tetrahydrofuran. The number-average molecular weights (M_n) of the polymers decreased with an increase in the M_2 fraction in the monomer feed. The degrees of polymerization decreased from 65.8, 103.7, and 51.4 to 21.9, 21.6, and 22.0 for polymers **2a**, **2b**, and **2c**, respectively. The higher and lower limits are intrinsic in the bis(4-vinylbenzoate)s and styrene, respectively, under the copolymerization conditions. The peaks due to the vinyl groups disappeared in the ^{13}C NMR spectrum of polymer **2b**, and thus, monomer **1b** was suggested to polymerize with complete cyclization. However, polymers **2a** and **2c** contained a small amount of residual double bonds. The extent of cyclization (f_c) was estimated from the area ratio between the peaks of the carbonyl and vinyl carbons in the inverse gated decoupling ^{13}C NMR spectra of polymers **2a** and **2c**. The f_c values for polymers **2a** and **2c** increased with increasing M_2 fraction. Hence, the cyclization tendency increased in the order of **1a** \approx **1c** < **1b**. The monomer reactivity ratio was $r_1 = 3.41$ and $r_2 = 0.38$ for **1a**, $r_1 = 3.81$ and $r_2 = 0.28$ for **1b**, and $r_1 = 1.97$ and $r_2 = 0.21$ for **1c**.

Chiroptical Properties. The chirality induction in the cyclocopolymerization systems should be confirmed by quantitative removal of the chiral templates from **2**. The ^1H NMR spectra of the resulting polymer **3** showed the complete removal of the chiral template (Figure 1). Even after removal of the chiral templates, polymer **3**

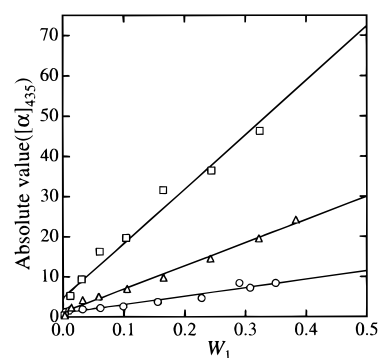


Figure 2. Specific optical rotations ($[\alpha]_{435}^{24}$, c 1.0 in CHCl_3) vs weight fraction of isolated benzoate diad (W_1) in polymers **3a** (\circ), **3b** (\square), and **3c** (\triangle). The W_1 values were calculated according to eq 1.

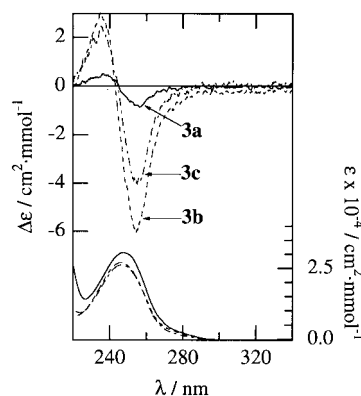


Figure 3. CD spectra of polymers **3a** ($f_1 = 0.11$, solid line), **3b** ($f_1 = 0.49$, short broken line), and **3c** ($f_1 = 0.24$, broken line). The $\Delta\epsilon$ and ϵ values were based on the concentration of the methyl 4-vinylbenzoate diad unit.

exhibited the expected optical activity due to the main chain chirality.

The optical activities of polymer **3** increased with a decrease in the M_1 fraction in the copolymer and the specific rotations ($[\alpha]_{435}^{24}$, c 1.0 in CHCl_3) changed from -1 to -8° for **3a**, from 0 to -46° for **3b**, and from 0 to -24° for **3c**. These optical activities originated in the chiral configuration of the main chain possessing numerous asymmetric centers. A minimum chiral repeating unit is generated in a racemo diad of the M_1 unit separated by M_2 units, namely, the isolated benzoate diad. On the first-order Markov model and perfect cyclization, the weight fraction of the isolated benzoate diad (W_1) could be calculated as follows:⁷

$$W_1 = w_1 \left(\frac{[M_2]}{r_1[M_1] + [M_2]} \right)^2 \quad (1)$$

w_1 is the weight fraction of the M_1 unit. Figure 2 shows the specific rotations of polymer **3** as a function of W_1 . Each of the copolymers showed a good linearity of the plots. This result means that the source of chirality in polymer **3** is attributed to the isolated benzoate diad. Here the slope of the plots gives the specific rotation per isolated benzoate diad. The CD spectra of polymer **3** showed the split Cotton effect with a negative first and a positive second Cotton effect (Figure 3). According to the exciton chirality method,⁸ these CD spectra indicate that the two methyl benzoate chromophores in the copolymer twist counterclockwise. Consequently, the CD spectra show that a segmental distribution with

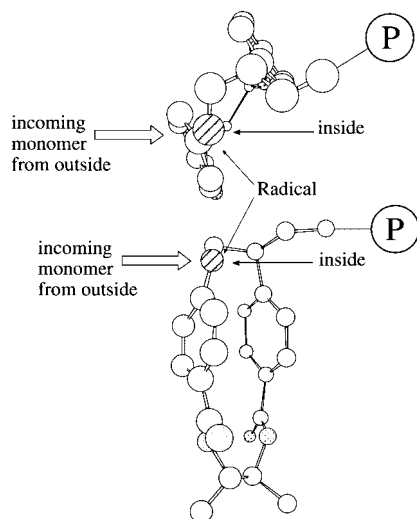


Figure 4. Cyclized radical structure of **6a** optimized using a semiempirical MO calculation. The atom with a slanted line indicates the radical center.

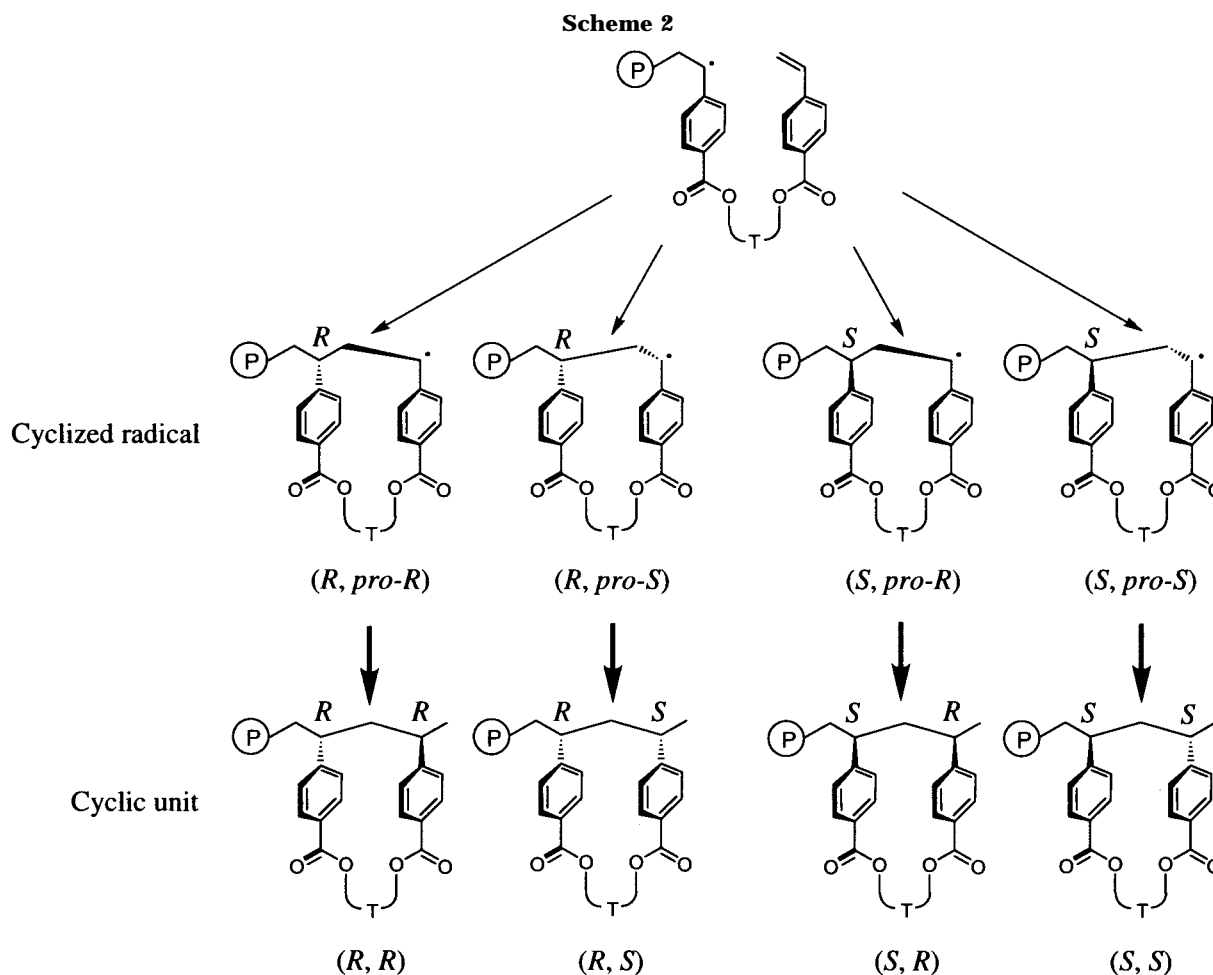
a high content of (*R,R*)-racemo benzoate diads is favored in polymer **3**. The templates having (*S,S*)-configuration thus induced the chirality of the (*R,R*)-racemo configuration in the main chain.

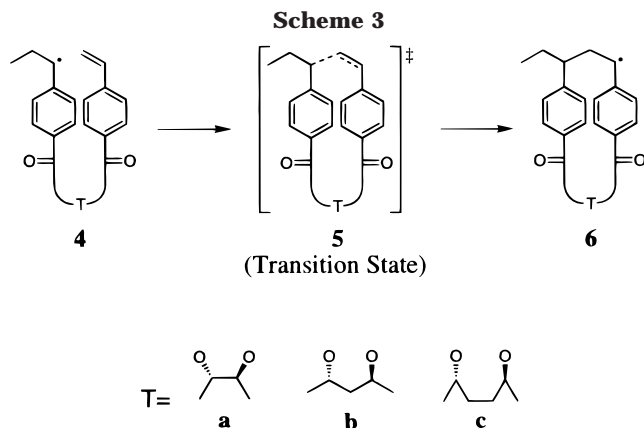
Model Reaction for Computation. As each of the intra- and intermolecular reactions induces new chirality, the structure of cyclic units in polymers **2** would consist of four stereoisomeric forms as shown in Scheme 2. The cyclized radical derived from **1a** stacks two

benzene rings in the molecule (Figure 4). The orbital of the radical is perpendicular to the benzene ring, which stabilizes the radical. One of the prochiral faces on the radical center is directed to the inside of the ring and the other to the outside of the ring. As the inside direction is effectively shielded by the benzene rings, the outside direction is favorable in the addition of monomers to the cyclized radical. Hence, the stereochemistry of the second chiral center is readied at the cyclization step. Consequently, the cyclization determines the stereoisomeric form in the cyclic units.

To characterize the transition state using computation, the cyclization is simplified as a reaction without the polymer chain (Scheme 3). For the first time, the conformation of the templates must account for this calculation. Templates **a**, **b**, and **c** are flexible to give a number of conformers in monomers **1a–c**. The major conformers in each monomer were estimated using a MM2 calculation (Figure 5).⁹ Template **a** predominately has a counterclockwise gauche form (hereinafter referred to as "*g*[−]") in the carbon skeleton, and template **b** substantially has a combination of the trans form ("*t*") and the clockwise gauche form ("*g*⁺"). In template **c**, the conformer is distributed into "*tg*⁺*g*⁺", "*g*⁺*tg*⁺", and "*ttt*" forms.

Having a high tendency for intramolecular cyclization, monomers **1a–c** should have a conformation suitable for the cyclization. For this reason, the conformers in Figure 5 can be applied to the conformation for **5a–c** in the transition state. The dissymmetric conformation such as "*tg*⁺" and "*tg*⁺*g*⁺" yields two directions for cyclization (Figure 6). Therefore, there are 4, 8, and





16 structures for **5a**, **5b**, and **5c**, respectively, in the transition state.

For the second time, the direction of the carbonyl groups must be considered, which is controlled by the chiral template. In monomers **1a–c**, the bond vectors of the two carbonyl groups are opposite in direction and each of the comonomers, except the “ttt” form, contains carbonyl groups where their *Si* faces are directed toward the inside. The “ttt” conformer contains the carbonyl groups having *Re* faces.

Stereochemical Distribution of the Cyclic Unit.¹⁰ The heat of formation of the transition state was estimated using the semiempirical MO calculation (Table 2). The reaction from **4** to **5** in Scheme 3 contains the paths leading to four stereoisomeric forms in the same manner as the four paths in Scheme 2. Since these paths are initiated from an identical reactant, the difference in the heat of formation at the transition state between the two paths equals that in the energy of activation. The chiral cyclic unit with (*R,R*)-configuration, thus, was produced through a lower activation energy path than that with the (*S,S*)-configuration except for the “ttt” conformer of **4c**. The results in which **4a**, **4b**, and **4c** favorably cyclize to form the (*R,R*)-racemo configuration are consistent with the experimental results of monomers **1a**, **1b**, and **1c**. The stereochemical distributions were also calculated (Table 3). The population excess of (*R,R*)-racemo cyclic units over (*S,S*)-racemo cyclic units for **6b** is greater than that for **6a**. Hence, template **b** is more effective for chirality induction than template **a**, which fact also agrees with the experimental result. Monomer **1c** leads to the formation of (*R,R*)-racemo cyclic units in the “tg⁺g⁺” and “g⁺tg⁺” conformers but to that of (*S,S*)-racemo units in the “ttt” conformer. Thus, a wide distribution of conformers lowered the chirality induction efficiency of **1c**. Consequently, a key to the excellent template is the higher selectivity between two racemo units and the larger depression of meso units.

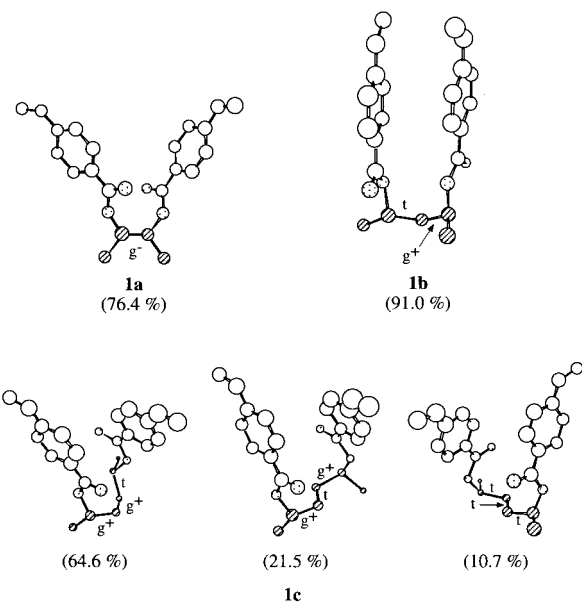


Figure 5. Major conformers of **1a**, **1b**, and **1c** estimated using a MM2 calculation.

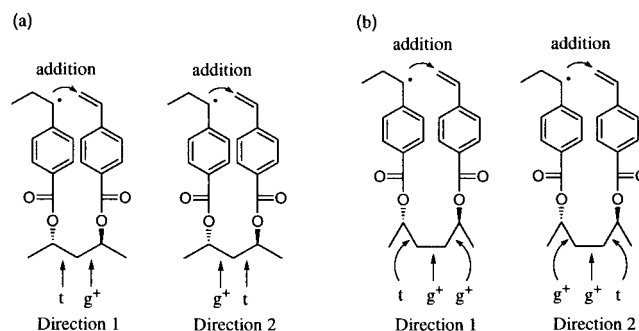


Figure 6. Direction of cyclization in the dissymmetric conformers.

The semiempirical molecular orbital calculations give absolute ratios of diastereomers in the model reactions. The intra- and intermolecular reactions induce the first and second chiral centers. The stereoselectivity of the chiral center, i.e., the diastereomeric excess (de) may be expressed as in eq 2 and 3 and for the first and second

$$\text{de (\%)} = \left| \frac{[(R,R) + (R,S)] - [(S,S) + (S,R)]}{[(R,R) + (R,S)] + [(S,S) + (S,R)]} \right| \times 100 \quad (2)$$

$$\text{de (\%)} = \left| \frac{[(R,R) + (S,R)] - [(S,S) + (S,R)]}{[(R,R) + (S,R)] + [(S,S) + (S,R)]} \right| \times 100 \quad (3)$$

chiral centers, respectively. The first center ranged

Table 2. Calculated Heat of Formation (kcal·mol⁻¹) of the Transition States in the Cyclization Using AM1

conformation	direction ^a	stereochemistry of cyclized radical			
		(<i>R,pro-R</i>)	(<i>R,pro-S</i>)	(<i>S,pro-R</i>)	(<i>S,pro-S</i>)
5a	g ⁻	-87.99 (0.00) ^b	-86.80 (+1.19)	-88.78 (-0.79)	-86.94 (+1.05)
5b	tg ⁺	-97.22 (0.00)	-96.08 (+1.14)	-97.50 (-0.28)	-95.68 (+1.54)
	g ⁺ t	-97.11 (0.00)	-95.78 (+1.33)	-97.37 (-0.26)	-95.39 (+1.72)
5c	tg ⁺ g ⁺	-101.26 (0.00)	-100.19 (+1.07)	-101.56 (-0.30)	-99.85 (+1.41)
	g ⁺ g ⁺ t	-100.84 (0.00)	-99.65 (+1.19)	-101.05 (-0.21)	-99.14 (+1.70)
	g ⁺ tg ⁺	-105.17 (0.00)	-103.97 (+1.20)	-105.72 (-0.55)	-103.41 (+1.76)
	ttt	-102.75 (0.00)	-104.05 (-1.30)	-103.15 (-0.40)	-103.84 (-1.09)

^a The directions are defined by Figure 6. ^b The values in parentheses were differences from (*R,pro-R*).

Table 3. Calculated Distribution of the Cyclic Unit Stereochemistry Using AM1

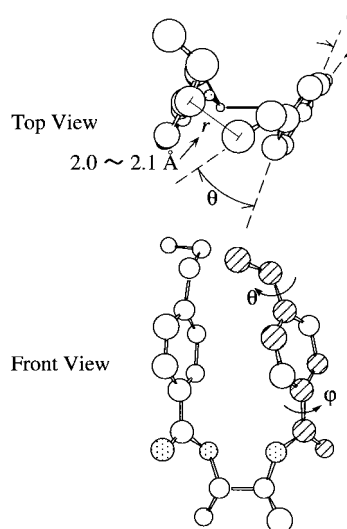
conformation	direction ^a	stereochemistry of cyclic unit				(R,R) - (S,S) ^b
		(R,R)	(R,S)	(S,R)	(S,S)	
6a	g ⁻	21.4	3.6	70.7	4.4	17.0
6b	tg ⁺	1	35.7	6.4	54.5	3.5
	g ⁺ t	2	37.2	5.0	55.1	2.8
6c	tg ⁺ g ⁺	1	34.6	6.9	54.4	4.1
	g ⁺ g ⁺ t	2	38.2	6.3	52.5	2.9
	g ⁺ tg ⁺		28.3	4.6	65.1	2.0
	ttt		6.6	47.1	12.1	34.3
						-27.7

^a The directions are defined by Figure 6. ^b Differences in population between (R,R)- and (S,S)-units.

from 7.4 to 50.0% de but the second one from 62.6 to 86.8% de, as calculated from the data in Table 3. The second center is more effective for stereocontrol than the first one. This conclusion drawn from the calculation coincides with Wulff's experimental derivation.³

Origin of Chirality Induction. The direction of the ester carbonyl groups in the monomer seriously affected the stereochemistry during the cyclization. When the carbonyl groups are situated each face to face with the *Si* face, the conformer leads to the formation of (R,R)-racemo cyclic units and *vice versa*. The cyclopolymerization process, therefore, is outlined on the basis of the results in this study (Scheme 4). The template controls the chiral orientation, namely, the *Re* or *Si* face with regard to the ester carbonyl groups in the monomer. The template having the (S)-configuration generally favors the *Si* face to give an enantiomeric cyclized radical. Further, the following intermolecular addition is controlled by the cyclized radical structure to give the cyclic unit with an (R,R)-configuration.

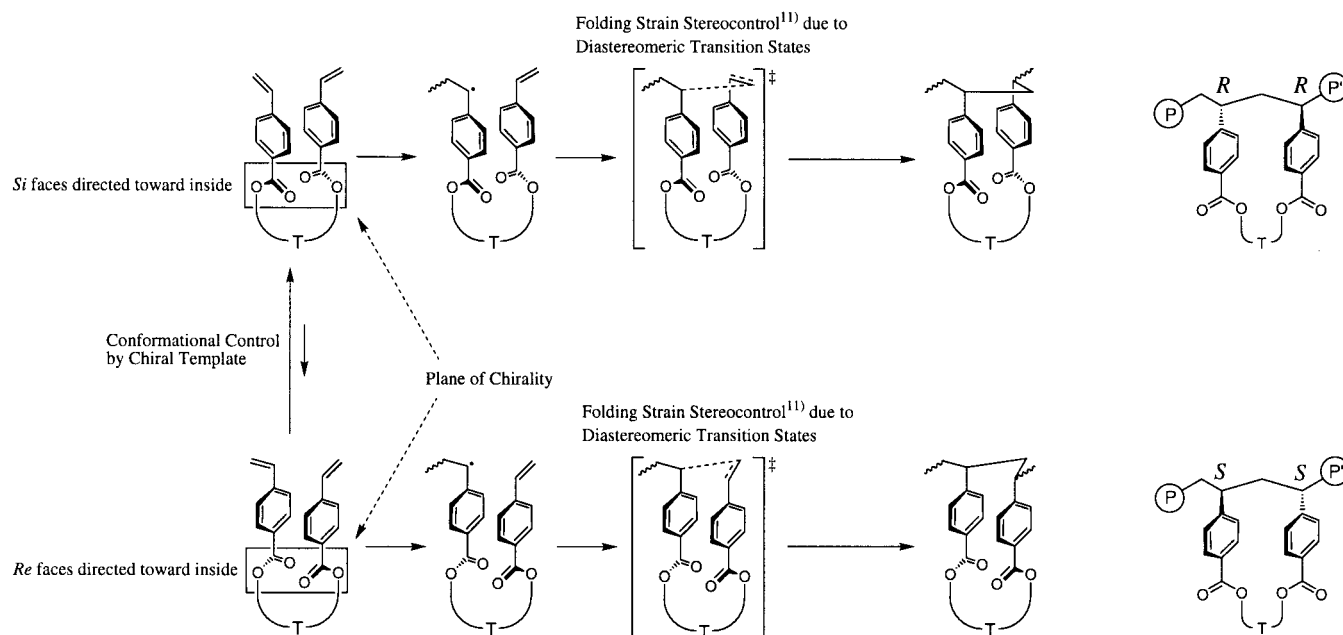
A path in which the transition state has a smaller deviation from coplanarity in the conjugated system of the vinylbenzoates is selected to form the (R,R)- or (S,S)-racemo cyclic units. In the cyclization, the rotation around a single bond occurs to release the strain energy on the stretched bonds and/or bent bond angles. On the other hand, the rotation which reduces the coplanarity is contrary to the stabilization in the transition state.

**Figure 7.** Structure **5a** (transition state) estimated using a semiempirical MO calculation (AM1 calculation). Torsion angles θ and ϕ are listed in Table 4.**Table 4. Torsion Angles θ , ϕ at the Transition State Calculated Using AM1^a**

conf	direction ^b	θ , deg		ϕ , deg	
		(R,pro-R)	(S,pro-S)	(R,pro-R)	(S,pro-S)
5a	g ⁻	-16.7	20.5	20.8	32.0
5b	tg ⁺	-15.9	19.8	13.3	25.4
	g ⁺ t	-15.4	20.5	21.0	23.9
5c	tg ⁺ g ⁺	-12.0	18.0	16.9	25.8
	g ⁺ g ⁺ t	-12.0	15.8	1.8	7.4
	g ⁺ tg ⁺	-9.0	15.2	8.0	19.3
	ttt	-17.3	15.3	-15.9	1.7

^a Torsion angles θ and ϕ are defined by Figure 7. ^b The directions are defined by Figure 6.

The torsion angles (θ and ϕ) of the transition state were estimated by the AM1 calculation (Figure 7 and Table 4). The transition state having the (R,R)-racemo configuration possessed a smaller torsional strain than that forming the (S,S)-racemo configuration, thus being advantageous in forming the (R,R)-racemo cyclic units.

Scheme 4

On the other hand, the "ttt" conformer was reversed. These results agreed very closely with those obtained by the heat of formation. The torsional strain in the transition state, which is essentially concerned with the heat of formation, should be closely connected with the origin of chirality induction during the cyclocopolymerization.

Conclusions

The chirality induction of a monomer having an acyclic chiral template was characterized by means of a semiempirical molecular orbital calculation. The AM1 calculation gave a result coinciding with the experimental ones for the bis(4-vinylbenzoate)s derived from (2*S*,3*S*)-2,3-butanediol and (2*S*,4*S*)-2,4-pentanediol templates. The 1,2- and 1,3-diols had a narrow distribution about the conformation and behaved as a rigid template. Because acyclic 1,4-diol was a flexible template, the monomer having (2*S*,5*S*)-2,5-hexanediol contained a conformer unsuitable for chirality induction because of the broad distribution of conformers, which fact disordered the stereoselectivity in the formation of the cyclic unit. In the transition state of cyclization, the deviation from coplanarity in the conjugated system was found to have an important connection with the heat of formation. The less deviation the conjugated system contained, the smaller the activation energy became. The chirality induction would result in the selection of a reaction path having less deviation from coplanarity.

References and Notes

- (1) Review: (a) Wulff, G. *Angew. Chem., Int. Ed. Engl.* **1989**, *28*, 21. (b) Okamoto, Y.; Nakano, T. *Chem. Rev.* **1994**, *94*, 349.
- (2) Configurationally: (a) Wulff, G.; Gladow, S.; Krieger, S. *Macromolecules* **1995**, *28*, 7434. (b) Wulff, G.; Gladow, S. *Macromol. Chem. Phys.* **1995**, *196*, 3341. (c) Wulff, G.; Gladow, S.; Kühneweg, B.; Krieger, S. *Macromol. Symp.* **1996**, *101*, 355. (d) Yokota, K.; Kakuchi, T.; Sakurai, K.; Iwata, Y.; Kawai, H. *Makromol. Chem., Rapid Commun.* **1992**, *13*, 343. (e) Kakuchi, T.; Haba, O.; Fukui, N.; Yokota, K. *Macromolecules* **1995**, *28*, 5941. (f) Haba, O.; Kakuchi, T.; Yokota, K. *Chirality* **1995**, *7*, 193. (g) Haba, O.; Morimoto, Y.; Uesaka, T.; Yokota, K.; Kakuchi, T. *Polymer* **1995**, *36*, 4151. (h) Kakuchi, T.; Haba, O.; Hamaya, E.; Naka, T.; Uesaka, T.; Yokota, K. *Macromolecules* **1996**, *29*, 3807. (i) Kakuchi, T.; Haba, O.; Uesaka, T.; Obata, M.; Morimoto, Y.; Yokota, K. *Macromolecules* **1996**, *29*, 3812. (j) Kakuchi, T.; Fukui, N.; Uesaka, T.; Obata, M.; Yokota, K. *Polymer* **1996**, *37*, 5703. (k) Kakuchi, T.; Haba, O.; Uesaka, T.; Yamauchi, Y.; Obata, M.; Morimoto, Y.; Yokota, K. *Macromol. Chem. Phys.* **1996**, *197*, 2931. (l) Uesaka, T.; Hamaya, E.; Haba, O.; Kakuchi, T.; Yokota, K. *Enantiomer* **1997**, *2*, 215. Conformationally: (m) Nakano, T.; Okamoto, Y.; Sogah, D. Y.; Zheng, S. *Macromolecules* **1995**, *28*, 8705.
- (3) Wulff et al. reported the diastereomer distribution in the radical cyclization of 3,4-*O*-cyclohexylidene-D-mannitol 1, 2; 5,6-bis-*O*-[(4-vinylphenyl)boronate] and 3,4-*O*-cyclohexylidene-D-mannitol 1, 2; 5,6-bis-*O*-[(4-vinylnaphthyl-1)boronate]. Wulff, G.; Kühneweg, B. *J. Org. Chem.* **1997**, *62*, 5785.
- (4) Lieser, J. K. *Synth. Commun.* **1983**, *13*, 765.
- (5) Allinger N. A. *J. Am. Chem. Soc.* **1977**, *99*, 8127.
- (6) MOPAC program version 6.01, JCPE No. 049, original source; QCPE No. 455 (MOPAC program version 6 for VAX workstations).
- (7) Ito, K.; Yamashita, Y. *J. Polym. Sci. Part A: Polym. Chem.* **1965**, *3*, 2165.
- (8) Harada, N.; Nakanishi, K. *Circular Dichroic Spectroscopy Exciton Coupling in Organic Stereochemistry*, Oxford University Press: Oxford, U.K., 1983.
- (9) Conformer distribution was calculated as follows: The set of initial structures for the MM2 calculation consisted of conformers having the staggered form of carbons in the template and was assembled by consideration of all combinations that could face the prochiral carbonyl groups in the monomer (i.e. *Re-Re*, *Re-Si*, *Si-Re*, *Si-Si* faces). In this manner, the number of initial structures obtained is 12 for **4a**, 36 for **4b**, and 108 for **4c**. The optimization of the initial structure using the MM2 calculation gave a set of equilibrium structures and its steric energy. Then, the relative free energy of a conformer was estimated using the steric energy as the enthalpy term and the symmetry number as the entropy term. The conformer distribution was calculated according to the Boltzmann distribution using the free energy at 333 K.
- (10) In most case, attempts using the reaction coordinate method failed for the transition state of the large cyclic structure. Then, the transition state was estimated as follows: The initial structure in which the distance of atoms involved in the radical addition was fixed at 2.0 Å was optimized using the semiempirical MO calculation. Further, this structure was fully optimized using NLLSQ algorithm. To confirm the transition state, the resulting structure was examined by normal coordinate analysis and the intrinsic reaction coordinate (IRC) calculation.
- (11) Tokoroyama, T. *J. Synth. Org. Chem., Jpn.* **1996**, *54*, 586.

MA971907T